CHAPTER IV

MANUSCRIPT

Chemical oxidation polymerization and characterization of poly ortho-anisidine nanoparticles

Kiattipong Khamngoen, Anuvat Sirivat*

The Petroleum and Petrochemical College, Chulalongkorn University, Bangkok, Thailand 10330

Abstract

Poly o-anisidine (POA) is a conductive polymer that can conduct electrons by a π-conjugated system. POA is a derivative of polyaniline, however, it still exhibits low electrical conductivity. This work is focused on the improvement of electrical conductivity of POA by synthesizing POA in nanoparticle forms using an anion as dopant. POA nanoparticles were obtained by chemical oxidation polymerization using anammonium persulfate as an oxidant and a sodium dodecyl sulfate (SDS) as a surfactant template for controlling size and shape of POA. The properties of the POA nanoparticles were characterized by fourier transform infrared spectroscopy, ultraviolet-visible absorption spectroscopy, thermal gravimetric analyzer, and scanning electron microscopy. The POA nanoparticles shapes were nano-fibers with diameter varying diameter from 63 to 129 nm depending on the polymerization temperature, polymerization time, and SDS concentration. The electrical conductive obtained varied from 0.022 to 198 S/cm, a variation of 4 orders of magnitude, depending on the POA nanoparticle size. The smallest POA nanoparticle size provided the highest electrical conductivity because of the larger surface area. Thus, this work show the higher electrical conductivity of the synthesized nano-fiber shape of POA which have not previously been reported elsewhere.

*Corresponding author: email: Anuvat.s@chula.ac.th;Tel.: +662 218 4131; Fax: +662 611 7221.

1.Introduction

Polymers are mostly used for insulator applications. While some of them can be classified as semiconductors because of their electrical conductivity (Dai *et al.*, 2004). A conductive polymer allows the electron transfer because its structure consists of the conjugated bonds (alternating single and double bonds or conjugated segments coupled with atoms providing p-orbitals for a continuous orbital overlap) which provides electron mobility (Heeger *et al.*, 2000). Examples of conductive polymers are polyaniline (Ozyilmaz *et al.*, 2010), polypyrrole (Tatyana *et al.*, 1997), and polyacetylene (Shirakawa *et al.*, 1997).

A conductive polymer doped by a chemical doping agent possesses charge defects (polaron, bipolaron, and soliton) in its structure through a process which is called doping. These defects induce the charge to be stabilized on the polymer chain that can conduct electron (Dai *et al.*, 2004). The doping methods can be proceeded by chemical doping (partially oxidized or reduced by electron donors or electron accepters), electrochemical doping (applied DC power source) (Wankhede *et al.*, 2002), photo–doping, charge-injection doping, and non–redox doping (Dai *et al.*, 2004).

Poly *o*-anisidine (POA) is a one of conductive polymers, a derivative ofaniline; it can be synthesized by the electrochemical and chemical oxidation polymerizations (Mazrouaa, 2012). POA can be used as a biosensor (Valentini *et al.*, 2004), surface coating (Chaudhari *et al.*, 2007), gas separation (Chen *et al.*, 1997), and etc. Nevertheless, POA exhibits poor the electrical conductivity (10^{-3}-10^{-4} S/cm) (Khan *et al.*, 2009), this is the limitation for using POA in many applications.

There have been numerous reports on the synthesis of conductive polymers with nano–structures to improve the electrical conductivity because the nano–

structures increase accessible path ways for electrons transfer (Brüggemann *et al.*, 2006).

In this work, the synthesis of the nano–structure POA was carried out by chemical oxidation polymerization using sodium dodecyl sulfate (SDS) as a surfactant template. The synthesized POA was characterized by FT-IR, UV-vis, and TGA to confirm POA structure. The effects of polymerization temperature, polymerization time, and surfactant concentration were also investigated on the morphology and electrical conductivity of POA and shall be reported here.

2. Experimental

2.1 Materials

An *o*-anisidine, OA, (AR grade, Sigma-Aldrich) was used as a monomer. Ammonium persulfate, APS, (AR grade, Sigma-Aldrich) and hydrochloric acid, HCl, solution, 0.1 M (ACI Labscan) were used as an oxidant and a catalyst, respectively. Sodium dodecylsulfate, SDS, (AR grade, Loba Chemie) was used as a surfactant that used to control size of polymer particles. Deionized water, acetone (AR grade, ACI Labscan), methanol (AR grade, QRëC) were used as a solvent without further purification.

2.2 Synthesis of poly *o*-anisidne (POA)

POA was synthesized via a chemical oxidation polymerization (Mazrouaa *et al.*, 2012). APS, as an oxidizer (0.49 g), was dissolved in a HCl solution (0.1 M, 10 ml). An *o*-anisidine 0.52 g (0.0043 M) and SDS were dissolved in the HCl solution (0.1 M, 100 ml) at various mole ratios (mole SDS/mole OA) from 0.008 to 16. Then the APS solution was dropped into the monomer solution at 1.0 ml/min. The monomer solution and the APS solution were mixed at 3, 25, and 60 °C for 18, 48, and 72 h. The product was terminated and precipitated with methanol. The dark green POA product was filtered and washed with methanol, DI water, and acetone,

then it was dried at 50 °C for 72 h. The code name used in the POA synthesis is POA-time-temperature-SDS mole ratio.

2.3 Characterization

The functional groups of POA were investigated by a FT-IR spectrometer (Nicolet, Nexus 670). The FT-IR absorption peaks were taken with 64 scans, at the wavenumber between 400-4000 cm^{-1}, and with a resolution of 4 cm^{-1}. The sample was prepared by grinding POA with potassium bromide (dried at 100 °C for 24 h) then compressed to a pellet and inserted in a sample holder.

The absorption spectra of POA were investigated by UV-VIS absorption spectroscopy (UV-Tecan, Infinite M200) at wavelengths from 230 nm to 1200 nm to identify the POA structure.

The weight loss of volatile molecules, the amount of residual water, and the degradation temperatures of POA were investigated by a TGA analyzer (Perkin Elmer, Pyris Diamond). The samples were weighed in the range of 4-10 mg and loaded into an alumina pan. The thermograms of POA were obtained with a temperature scan from 25 °C to 600 °C at a heating rate of 10 °C/min under nitrogen atmosphere.

The morphology of POA was examined using a scanning electron microscope, SEM, (JEOL, JSM-5410LV). POA particles were placed on a carbon tape and coated with thin layer of gold prior to measurement. Magnifications were 20000x and 35000x operating at 15 kV of electrons beam.

2.4 Electrical conductivity measurement

Electrical conductivity of POA was measured by a custom-built two-point probe at room temperature and at 60 %RH. The sample was compressed to a pellet with a hydraulic compressor. The custom-built two-point probe was connected to a conductivity meter which measured the current that responded to an applied voltage. The specific conductivity (σ) was calculated by using Eq. (1);

$$\sigma = 1/\rho = 1/(R_s t) = I/(KVt) \tag{1}$$

where, σ is the specific conductivity (S/cm), ρ is the specific resistivity (Ω.cm), R_s is the sheet resistivity (Ω), I is the measured current (A), K is the geometric correction factor as calibrated by using standard silicon wafer sheets with known specific resistivity values, V is the applied voltage (V), and t is the film thickness (cm).

3. Results and discussion

3.1 Characterization

The FT-IR spectra of POA are shown in Figure 1. The peaks at 1579 and 1451 cm^{-1} are characteristics of the C=C stretching of the quinoniod and benzenoid rings, respectively (Mondal et al., 2006) corresponding to the POA structure o as shown in Figure 2. The peaks at 1289 cm^{-1}, 1198 cm^{-1}, 1166 cm^{-1}, and 1111 cm^{-1} are assigned to the C-N$^+$ stretching, the C-O aromatic stretching, the secondary aromatic amine stretching, and the C-O-C ether group stretching in aromatic ring, respectively (Wang et al., 2005; Khan et al., 2009; Khan et al., 2012; Pandey et al., 1993). Not only characteristic peaks of POA are visible in the IR spectra, but also characteristic peaks of SDS appear which confirm successfully doped POA by SDS. The FT-IR peaks of doped POA as similar to those of the dedoped POA except the peaks at 2928cm^{-1}, 1471cm^{-1}, 1224 cm^{-1}, 1087 cm^{-1}, and 846 cm^{-1} corresponds to the C–H stretching and bending, the S=O stretching vibration of SO$_4^-$ from SDS molecules, and the C–H stretching, respectively (Ramimoghadam et al., 2012).

UV-vis spectra of doped and dedoped POA are shown in Figure 3.The absorption peaks of dedoped POA are at 330 and 600 nm which can be referred to as the quinoniod and benzenoid structures (Figure 2). The absorption peak at 330 nm corresponds to the bonding to anti-bonding (π-π*) transition of the benzenoid ring (Kulkani et al., 2006), and the absorption peak at 600 nm corresponds to the transition from the non-bonding to anti-bonding orbital (n-π*) between the benzenoid and quinonoid rings (Patil et al., 1998). However, doped POA has the absorption

peaks at 330, 430, and 800 nm which are excitations of the polaron due to doping (Yang *et al.*, 1999).

The thermal behavior of POA shows 2 steps of weight loss as shown in Figure 4. First, the decomposition temperature is 100 °C resulting from the removal of water absorbed in the polymer. Secondly, the decomposition temperature of 370-500 °C corresponds to the decomposition of POA backbone (Mondal *et al.*, 2006). However, the decomposition temperature of doped-POA also exhibits the degradation of dopant (SDS) at 180-250 °C (Kulkani *et al.*, 2006). The degradation of dopant is consistent with the peak of SDS appearing in the FTIR spectra, thus SDS acted as a dopant on the POA structure as shown in Figure 5. APS acted as an oxidant and initiator creating OA cation radicals in the first step. Then, the POA polymeric chain was generated from the OA cation radicals to become a protonated dimer which subsequently was deprotonated. Finally, the POA polymer was doped by the sulfate ion of dodecyl sulfate of in the SDS solution.

3.2 Morphology

3.2.1 Effect of polymerization temperature

The morphology of POA synthesized based on the effect of reaction temperature as 3 and 25 °C is shown in Figure 6. The POA nanoparticles are granular and nano-fiber shapes with the sizes of 322 ± 65 nm and 129 ± 33 nm for 25 and 3 °C, respectively. The POA nanoparticle becomes more agglomerate with increasing reaction temperature because the higher reaction temperature accelerates the polymerization rate resulting in POA particle reaching their final more rapidly (Boguslavsky *et al.*, 2005; Huajing *et al.*, 2010).

3.2.2 Effect of polymerization time

The morphology of POA depends on the polymerization time as shown in Figure 7. The POA nanoparticle is of a fiber shape with the diameter of 129 ± 33 nm to 65 ± 8.6 nm. At the polymerization time of 48 h, the POA nanoparticle is the smallest (65 ± 8.6 nm) appearing as a full fiber. At the polymerization time of 18 h,

the POA nanoparticle is not a full fiber and POA nanoparticle size (129 ± 33 nm) is larger than that of 48 h. The less polymerization time provides the incomplete polymerization of POA. However, at the polymerization time of 72 h, larger POA nanoparticle (75 ± 14 nm) results because the polymer can grow to a longer chain length resulting in particle agglomeration (Boguslavsky *et al.*, 2005).

3.2.3 Effect of SDS concentration

The particles size of synthesized POA under the effect of SDS concentration varies between 60 ± 11 nm and 90 ± 18 nm and the particles shape varies from nonuniformed shapes to a nanofiber, as shown in Figure 8, at 0.012 to 12.00 mole ratios of SDS/OA. The SDS mole ratio that is suitable to produce POA into the full-nanofiber is at 8 SDS/OA mole ratios, and with the diameter of 65 ± 8.6 nm. At the 0.12 mole ratio of SDS/OA, the POA particle is the largest in the ununiformed shapes because SDS concentration is lower than that of CMC (CMC of SDS is 0.12 mole ratio of SDS/OA) and thus no micelle in the polymerization. At higher than CMC, POA forms a fiber shape due to the packing parameter. The micelle shape is identified by the packing parameter ($V_H/l_c a_0$) of micelle-solution. The structure of the micelle is cylindrical shape with the value of packing parameter in the range of 0.3-0.5 (Rosen *et al.*, 2004). The POA fiber becomes more agglomerated when the mole ratio of SDS/OA is 12:00. At a higher concentration of SDS, the amount of micelle increases and induces more micelle fusion resulting in the POA particle agglomeration (Paradee and Sirivat, 2013).

3.3 Electrical conductivity

The electrical conductivity increases from 8.8×10^{-2} S/cm to 193.44 S/cm depending on the SDS/OA mole ratio. The electrical conductivity of POA increases with increasing SDS mole ratios until SDS mole ratio reaches to 8.00, the highest conductivity, and then the electrical conductivity decreases (Figure 9) because SDS acted as a dopant (Tadros *et al.*, 2009). SDS consists of an anion of sulfate group, it can induce the structure of POA to have more conjugated double bonds as shown in

Figure 5. At the SDS mole ratio higher than 8.00, the electrical conductivity decreases because the reaction of self-screening occurs on the polymerizing and doping by SDS anions. The electrical conductivity not only depends on doping level but also depends on morphology. Magnitude of the highest electrical conductivity is 193.44 S/cm at SDS/OA mole ratio of 8.00. This ratio provides a full fiber in polymer morphology (with a diameter of 63 ± 9 nm) and the highest electrical conductivity (193.44 S/cm) because of the higher surface area for electrons to transfer.

Compared with Wang *et al.* synthesized POA by chemical oxidation polymerization, APS was used as the oxidant and methane sulfonic acid (MSA), hydrochloric acid (HCl), and p-toluene sulfonic acid (pTSA) were used as the dopants. pTSA provided the highest electrical conductivity when compared with HCl and MSA because the molecular structure of pTSA could stabilize the bond between the dopant and the polymer chain through the benzene ring of the dopant anion that assisted formation of a resonance structure for electrons to flow over the entire polymer chain. Jadhav *et al.* synthesized POA with SDS as a surfactant. The morphology of polymer was rod-shaped with a particle size between 40 nm to 50 nm because SDS created the cylindrical micelle resulting in rod-shaped of nano-size POA.

Thus, the morphology and electrical conductivity of POA depend on the polymerization conditions such as temperature and time of polymerization, surfactant concentration, and characteristics of dopant. In addition, the electrical conductivity can be directly related to the morphology and particle size of POA.

3.4 Reproductivity

POA synthesis in condition of 48 hrs, 3 °C, and 8 mole ratio of SDS: *o*-anisidinemonomer can reproduce which the POA properties as electrical conductivity (144.47 ± 72.83 S/cm) and the POA characteristic as chemical properties (FT-IR, UV-vis, H^1-NMR), thermal property (TGA), and morphology (cylindrical shape, 77 ± 17.7 nm) are similar.

4. Conclusion

In the present study, POA nanoparticles were successfully synthesized using APS as an oxidant and SDS as a surfactant platform in the chemical oxidation polymerization in the range of 63 to 129 nm depending on the polymerization temperature, polymerization time, and SDS concentration. The synthesis produced POA nanofibers. The POA nanofiber size increased with increasing polymerization time and SDS concentration because these factors controlled the polymerization rate and created particle agglomeration and particle connection together. The electrical conductivity of POA increased from 0.025 to 193.44 S/cm with decreasing POA nanoparticle size. The condition that generated the highest conductivity (193.44 S/cm) with connected nano-fiber (65 ± 8.6 nm) was POA synthesized using 8:00 mole ratio of SDS at 3 °C for 48 h.
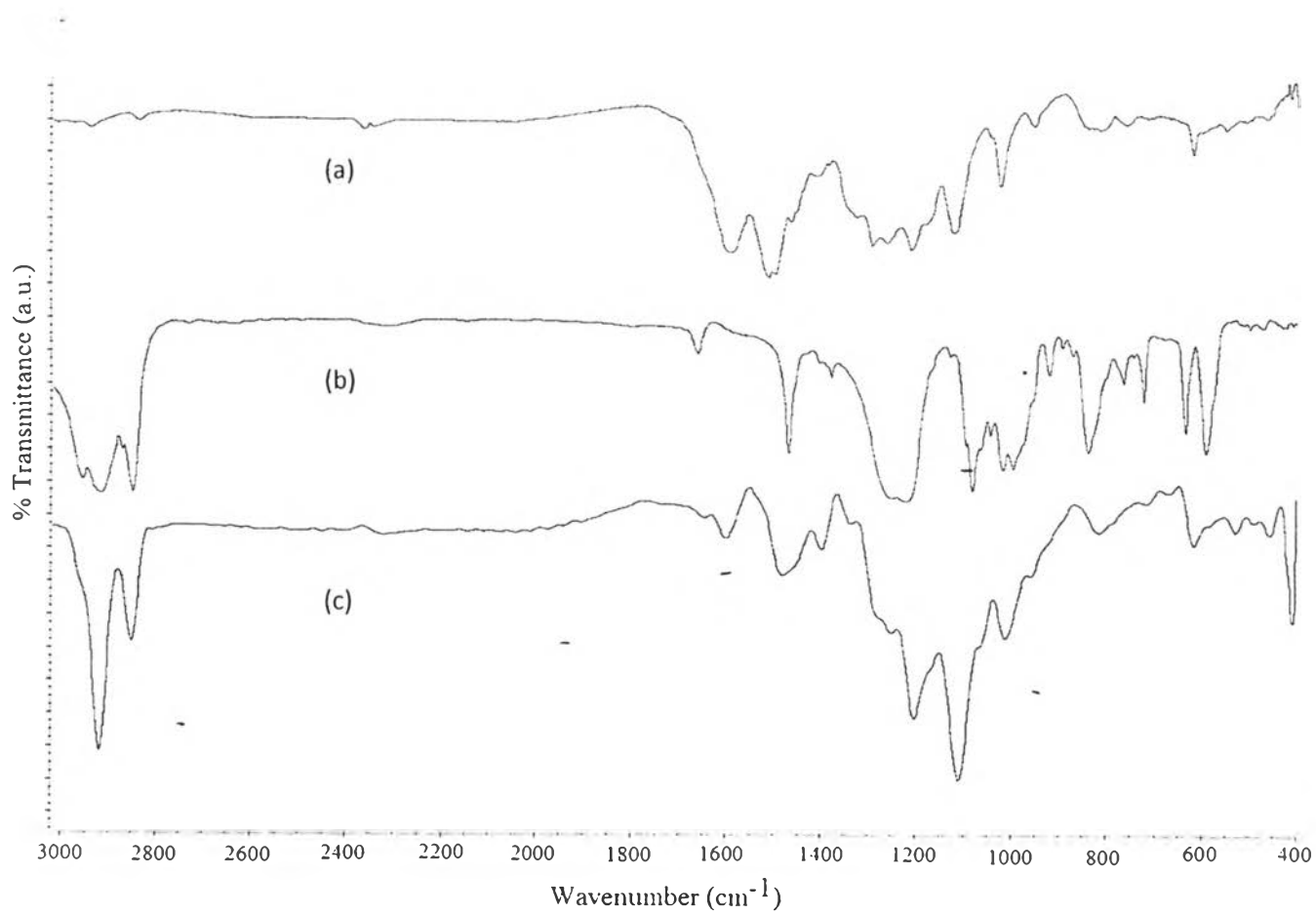
Acknowledgement

Figure 1 FTIR spectra of POA: (a) dedoped POA; (b) SDS; and (c) doped POA.

Figure 2 Chemical structure of quinoniod (a) benzenoid and (b) ring of POA (Kulkarni *et al.*, 2006).
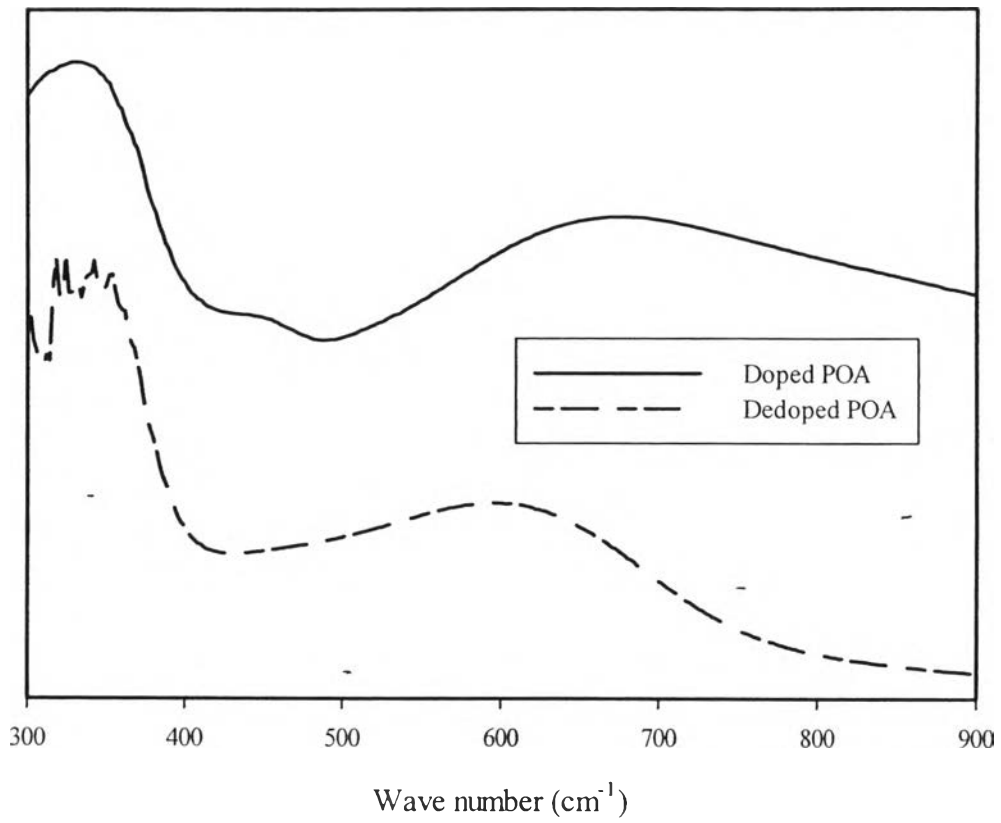
Wave number (cm^{-1})

Figure 3 UV-vis spectra of POA.
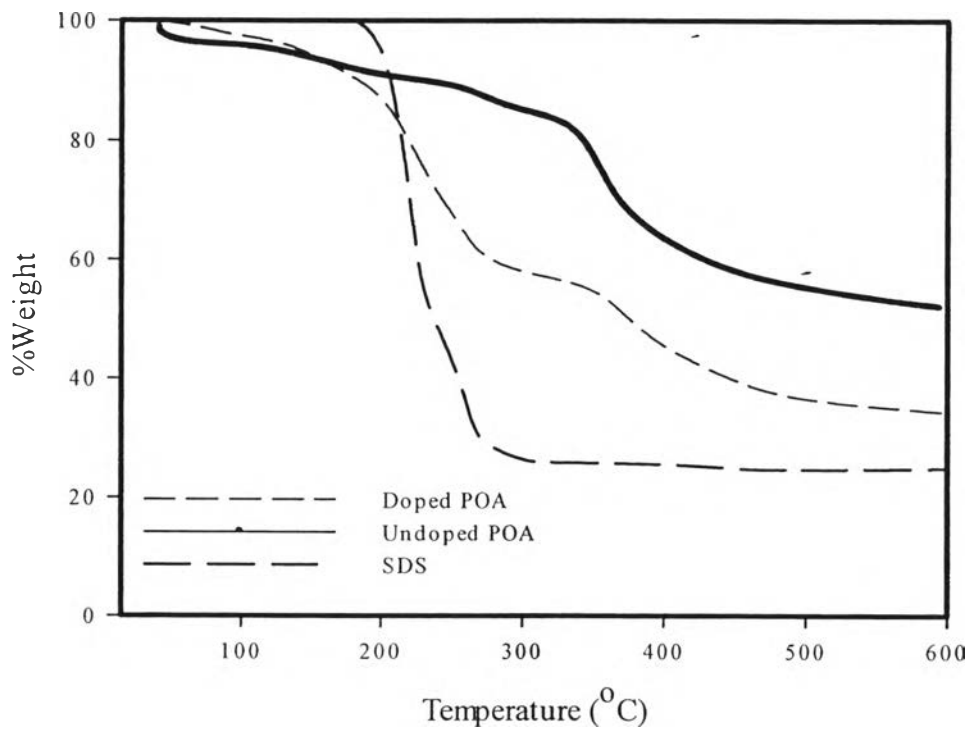

Temperature (^{o}C)

Figure 4 Thermogram of POA.
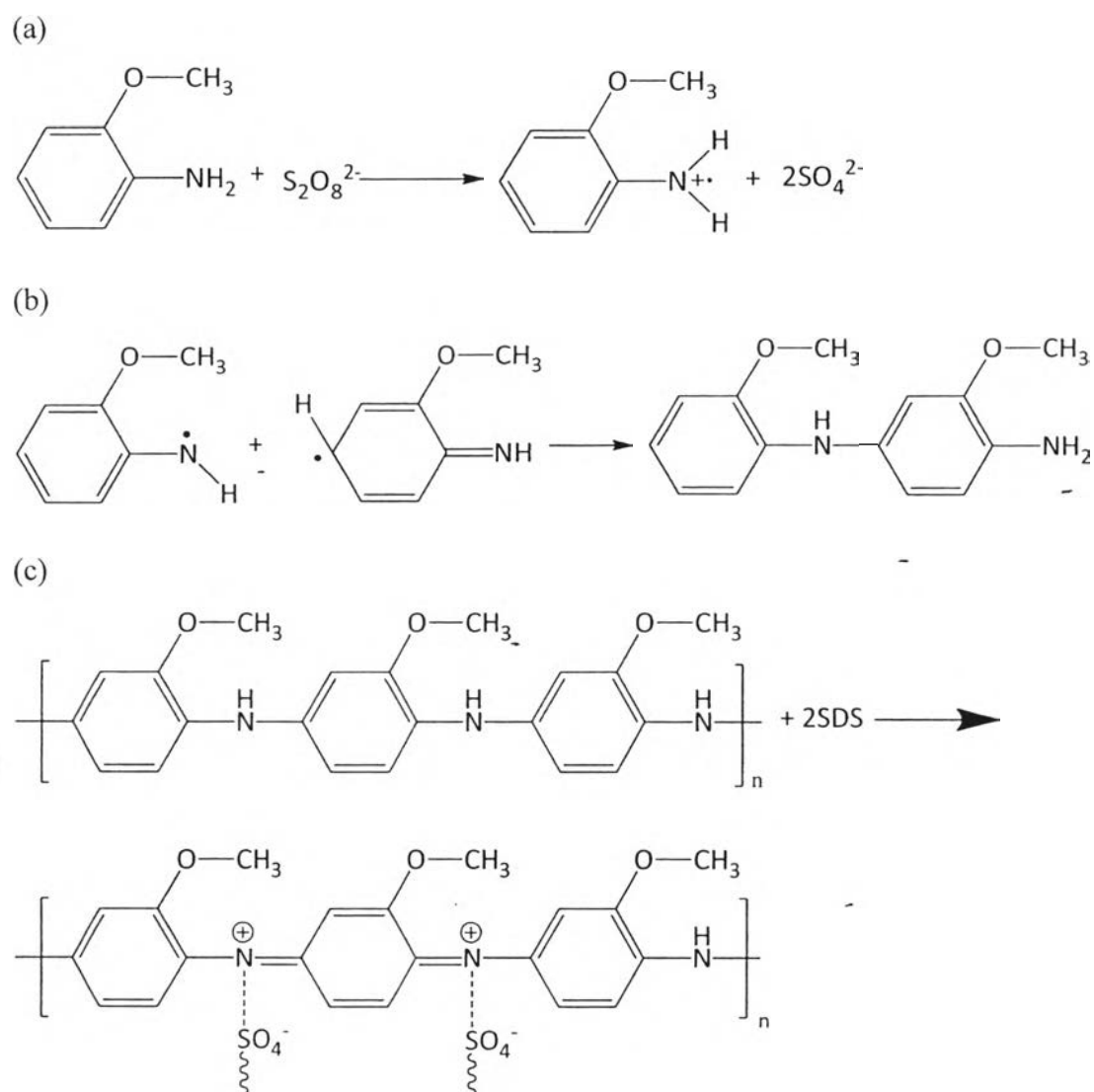
(a)

(b)

(c)

Figure 5 Proposed polymerization mechanism of POA: (a) OA as monomer is oxidized by APS to a cation radical; (b) OA cation radicals form dimers that subsequently get deprotonated; and (c) POA polymer is doped and dodecyl sulfate ion acts as counter ion (Khan *et al.*,2009).
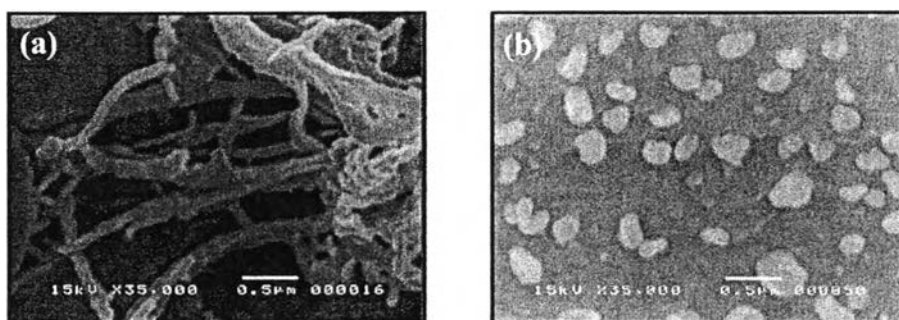
Figure 6 Morphology of POA nanoparticles prepared using various synthesis temperature: (a) 3 °C and (b) 25 °C.
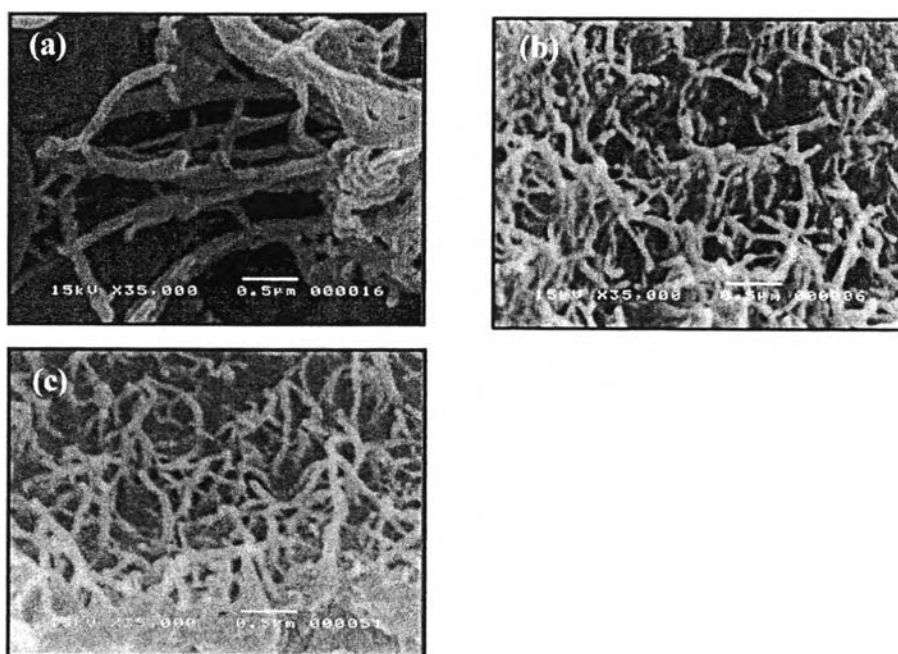

Figure 7 Morphology of POA nanoparticles prepared using various synthesis times: (a) 18h; (b) 48h; and (c) 72h.
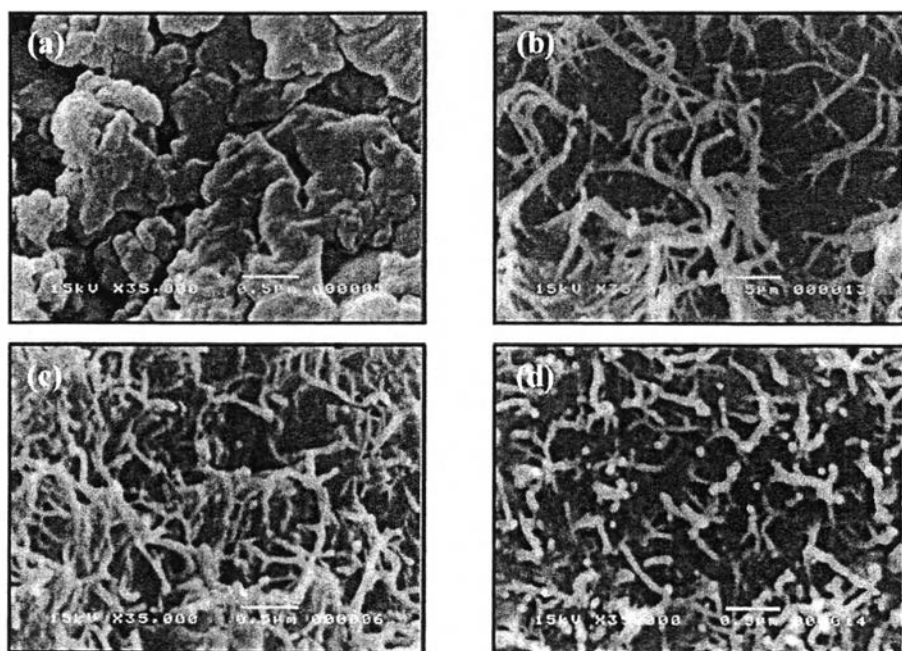
Figure 8 Morphology of POA nanoparticles prepared using various SDS mole ratios: (a) 0.12; (b) 4.00; (c) 8.00; and (d) 12.00.
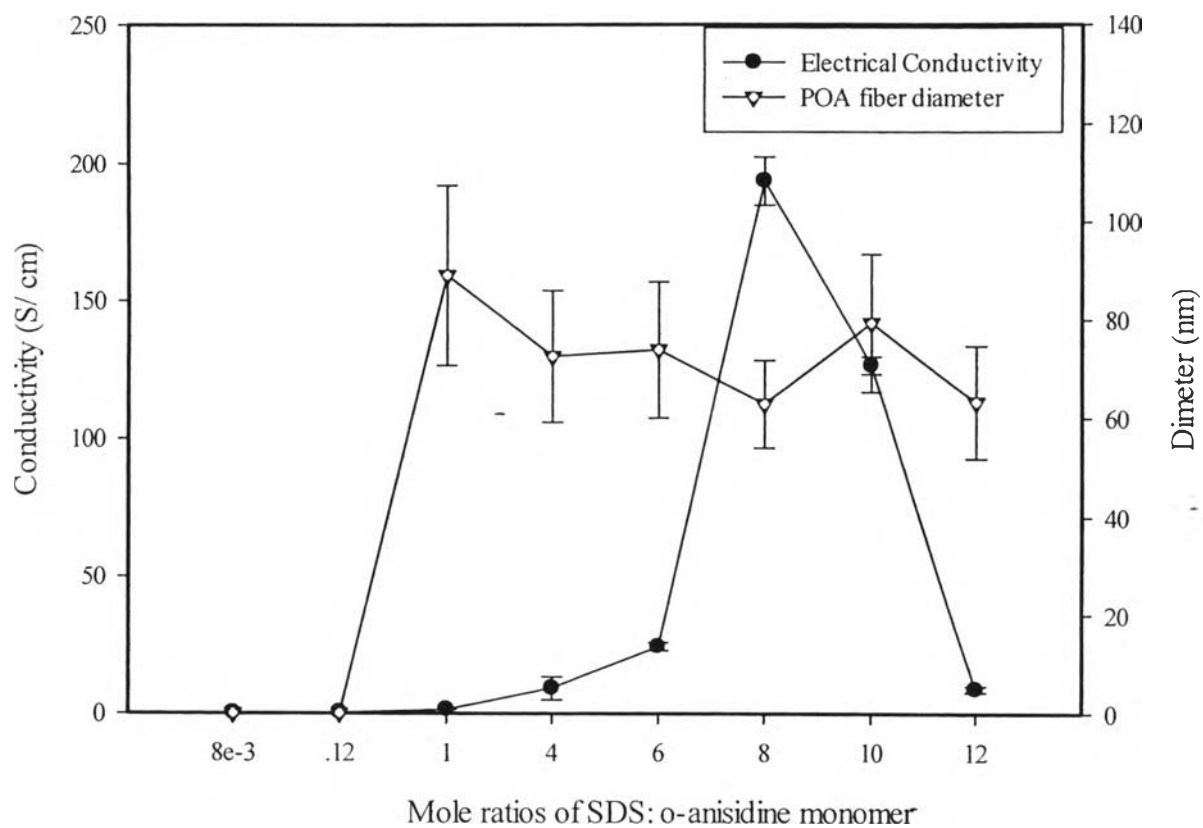
Figure 9 Electrical conductivity and fiber diameter of poly *o*-anisidine at various mole ratios of SDS: *o*-anisidine monomer.

Table 1 Comparison of particle size, particle shape and electrical conductivity of POA obtained under various synthesis conditions

Synthesis method	Particle size (nm)	Shape	Electrical conductivity (S/cm)	Remarks*
Emulsion polymerization (SDS as surfactant)	-	Lamellar	$8.85 \pm 0.03 \times 10^{-2}$	OA:SDS = 1:0.008
	-	Lamellar	$1.66 \pm 0.01 \times 10^{-1}$	OA:SDS = 1:0.12
	90 ± 17.9	Fiber agglomerate	1.35 ± 0.03	OA:SDS = 1:1
	73 ± 13.1	Fiber agglomerate	9.05 ± 2.93	OA:SDS = 1:4
	73 ± 13.5	Fiber agglomerate	24.19 ± 1.07	OA:SDS = 1:6
	65 ± 8.6	Fully formed Fiber	193.44 ± 6.21	OA:SDS = 1:8
	80 ± 13.7	Fiber agglomerate	126.23 ± 2.24	OA:SDS = 1:10
	60 ± 11.2	Fiber agglomerate	8.66 ± 0.79	OA:SDS = 1:12
Chemical oxidation polymerization (Wang et al., 2011)	-	Spherical	$1.8 \pm 0.2 \times 10^{-3}$	OA:MSA = 1:1.25
	-	Plate-like	$8.4 \pm 0.8 \times 10^{-3}$	OA:pTSA = 1:1.25
	-	Spherical	$2.5 \pm 0.1 \times 10^{-3}$	OA:HCl = 1:1.25
Emulsion polymerization (SDS as surfactant) (Jadhav et al., 2009)	40 – 50	rod-shaped	-	OA:SDS = 1:7.9

*Ratios given are mole ratios

References

Alan , J., Heeger Alan ,G. ,MacDiarmid Hideki ,Shirakawa (2000). Conductive polymers. The Nobel Prize in Chemistry, 2000: Conductive polymers. Bengt Nordén, E.K. Sweden.

Boguslavsky, L., Baruch, S. and Margel, S. (2005). Synthesis and characterization of polyacrylonitrile nanoparticles by dispersion/emulsion polymerization process. Journal of Colloid and Interface Science 289(1), 71-85.

Brüggemann, B., Organero, J.A., Pascher, T., Pullerits, T. and Yartsev, A. (2006). Control of Electron Transfer Pathways in a Dye-Sensitized Solar Cell. Physical Review Letters 97(20), 208301.

Chaudhari, S. and Patil, P.P. (2007). Corrosion-protection aspects of electrochemically synthesized poly(o-anisidine) coatings on mild steel: An electrochemical impedance spectroscopy study. Journal of Applied Polymer Science 106(1), 400-410.

Chen, Z.-k., Ng, S.-c., Li, S.F.Y., Zhong, L., Xu, L. and Chan, H.S.O. (1997). The fabrication and evaluation of a vapour sensor based on quartz crystal microbalance coated with poly(o-anisidine) langmuir一€"blodgett layers. Synthetic Metals 87(3), 201-204.

Dai, L. (2004). Intelligent Macromolecules. Intelligent Macromolecules for Smart Devices, Springer London: 81-116.

Jadhav, R.S., Hundiwale, D.G. and Mahulikar, P.P. (2010). Synthesis of nano polyaniline and poly-o-anisidine and applications in alkyd paint formulation to enhance the corrosion resistivity of mild steel. J. Coat. Technol. Res. 7(4), 449–454.

Khan, A.A., Habiba, U. and Khan, A. (2009). Synthesis and Characterization of Organic-Inorganic Nanocomposite Poly-o-anisidine Sn(IV) Arsenophosphate: Its Analytical Applications as Pb(II) Ion-Selective Membrane Electrode. Int J Anal Chem.

Khan, A.A. and Khan, A. (2009). Synthesis, characterization and electrical conductivity measurement studies of poly-o-anisidine Sn(IV) phosphate [POASn(IV)P] nano-composite cation-exchange material. Materials Science and Engineering: B 158(1-3), 92-97.

Khan, A.A., Shaheen, S. and Habiba, U. (2012). Synthesis and characterization of poly-o-anisidine Sn(IV) tungstate: A new and novel organic inorganic nano-composite material and its electro-analytical applications as Hg(II) ion-selective membrane electrode. Journal of Advanced Research 3(3), 269-278.

Kulkarni, M.V., Viswanath, A.K. and Khanna, P.K. (2006). Synthesis and Characterization of Poly(o-anisidine) Doped with Polymeric Acids. International Journal of Polymeric Materials and Polymeric Biomaterials 55(7), 501-512.

Mansour, N., Mohamed, M., Abed, M.Y. and Mazrouaa, A.M. (2012). Thermal and electrical properties of nanocomposite poly o-anisidine/metal oxides. High Performance Polymers.

Mazrouaa, A.M., Abed, M.Y., Mansour, N.A. and Mohamed, M.G. (2012). Synthesis and Characterization of Poly O-Anisidine Nanoparticles and their Nanocomposite. Material Sciences & Engineering 1(1).

Mondal, R.A., Dongre, S.P., Mahatme, U.B., Tabhane, V.A., Hedau, M.J. and Kondawar, S.B. (2006). Studies on chemically synthesized doped poly(o-anisidine) and copoly{aniline-(o-anisidine)}. Modern Physics Letters B 20(23), 1461-1470.

Ozyilmaz, A.T., Ozyilmaz, G. and Yigitoglu, O. (2010). Synthesis and characterization of poly(aniline) and poly(o-anisidine) films in sulphamic acid solution and their anticorrosion properties. Progress in Organic Coatings 67(1), 28-37.

Pandey, S.S., Annapoorni, S. and Malhotra, B.D. (1993). Synthesis and characterization of poly(aniline-co-o-anisidine). A processable conducting copolymer. Macromolecules 26(12), 3190-3193.

Patil, S., Mahajan, J.R., More, M.A., Patil, P.P., Gosavi, S.W.and Gangal, S.A. (1998). Electrochemical polymerization of poly(o-anisidine) thin films: effect of synthesis temperature studied by cyclic voltammetry. Polymer International 46(2), 99-105.

Ramimoghadam, D., Hussein, M.Z. and Taufiq-Yap, Y.H. (2012). The Effect of Sodium Dodecyl Sulfate (SDS) and Cetyltrimethylammonium Bromide (CTAB) on the Properties of ZnO Synthesized by Hydrothermal Method. Int J Mol Sci.

Rosen, M.J. (2004). Micelle Formation by Surfactants. Surfactants and Interfacial Phenomena, John Wiley & Sons, Inc.: 105-177.

Shirakawa, H., Louis, E.J., MacDiarmid, A.G., Chiang, C.K. and Heeger, A.J. (1977). Synthesis of electrically conducting organic polymers: halogen derivatives of polyacetylene, (CH). Journal of the Chemical Society, Chemical Communications(16), 578-580.

Tadros, T.F. (2009). Physical Chemistry of Surfactant Solutions. Colloids in Agrochemicals, Wiley-VCH Verlag GmbH & Co. KGaA: 19-40.

Tat'yana, V.V. and Oleg, N.E. (1997). Polypyrrole: a conducting polymer; its synthesis, properties and applications. Russian Chemical Reviews 66(5), 443.

Valentini, L., Bavastrello, V., Stura, E., Armentano, I., Nicolini, C. and Kenny, J.M. (2004). Sensors for inorganic vapor detection based on carbon nanotubes and poly(o-anisidine) nanocomposite material. Chemical Physics Letters 383(5 1€"6), 617-622.

Wang, G., Wang, L. and Li, X. (2005). Synthesis and characterization of poly(o-anisidine)/V2O5 and poly(o-anthranilic acid)/V2O5 nanocomposites. Polymer International 54(7), 1082-1087.

Wang, X., Ray, S., Gizdavic-Nikolaidis, M. and Easteal, A.J. (2011). The effects of dopant acids on structure and properties of poly(o-methoxyaniline). Journal of Polymer Science Part A: Polymer Chemistry 50(2), 353-361.

Wankhede, M.G., Koinkar, P.M., More, M.A., Patil, P.P. and Gangal, S.A. (2002). Synthesis of poly(O-anisidine) coatings on low carbon steel by electrochemical polymerization of O-anisidine. Advances in Polymer Technology 21(1), 33-43.

Yang, C., Fang, Z. and Zhang, P. (1999). UV-Vis spectra of polyaniline doped with camphor sulfonic acid in different organic solvents. Journal of Central South University of Technology 6(2), 127-129.